Can HCCH/HBNH break B=N/C=C bonds of single-wall BN/carbon nanotubes at their surface?

Tapas Kar[1]*, Peter Grüninger[2], Steve Scheiner[1], Holger F. Bettinger[2] and Ajit K. Roy[3]

[1]Department of Chemistry and Biochemistry, Utah State University, Logan, UT 84322-0300, United States
[2]Institute for Organic Chemistry, University Tübingen, Auf der Morgenstelle 18, 72076 Tuebingen, Germany
[3]Materials and Manufacturing Directorate, Air Force Research Laboratory, Wright-Patterson Air Force Base, OH 45433, United States

Abstract

The iminoborane (HBNH) molecule, which prefers cycloaddition reactions, selectively breaks a B=N bond of smaller diameter single-wall BNNTs and expands a ring at their surface, either at the edges or at the middle of the tube. Density functional theory (DFT) is used to test whether its organic counterpart HCCH can do the same with BNNTs. HCCH-BNNT complexes are identified and transition states located for these combination reactions. Also explored are possible reactions of HBNH with SWNTs and HCCH with SWNTs. Data suggest that B=N (C=C) bond breaking, followed by ring expansion at the surface may be possible. Although [2+2]cycloaddition reaction seems possible for HBNH-BNNTs, a high energy barrier hinders the process for other combinations of host and guest. Introduction of substituents to HBNH/HCCH may allow a facile process. In most cases of HCCH-BNNTs, HBNH-SWNTs, and HCCH-SWNTs, transition states are identified and suggest an electron-rich guest might lower barrier heights to form stable complexes. Reaction with HCCH or HBNH at the bay-region of smaller diameter armchair tube is not favorable.

Corresponding author: Email: tapas.kar@usu.edu, Fax: 1-435-797-3390

Introduction

A new feature of reactivity of iminoborane (HBNH), the inorganic counterpart of acetylene (HC≡CH), at the surface of boron nitride nanotube has recently been revealed by theoretical investigation [1]. In general, iminoborane and its derivatives readily oligomerize to stable cyclic $(RBNR')_n$ (n =2,3 and 4) products [2-5]. However, when allowed to interact with boron nitride nanotubes [6-12], HBNH not only selectively breaks the B=N double bond of the single-wall BN nanotubes (BNNTs) but also expands the hexagonal BN-network of the tube to larger cages at the surface. Such expanded structures are stabilized by 30-50 kcal/mol depending on the chiral vector and reactive site of the tube. Complexation energy decreases with diameter of the tube and is lowest for a planar BN-sheet. These findings suggest that the structural strain integral to smaller diameter tubes helps to facilitate bond breaking/ring expansion reactions with HBNH. In addition to such activity, HBNH also undergoes [2+2]cycloaddition at certain sites of the BNNT which is energetically less favorable than cleavage/expansion. Low barrier heights (less than 14 kcal/mol) for bond cleavage/ring expansion indicate such chemical modification of BNNT at the surface by HBNH molecule may be realized in experiment.

The organic counterpart of iminoborane, acetylene (HCCH) is one of the key precursors [13-15] in a large range of chemical vapor deposition (CVD) processes to grow single-wall carbon nanotubes (SWNTs). Recent studies [16-19] by Scott's group opens a new dimension of activity of acetylene on developing SWNTs from polycyclic aromatic hydrocarbon (PAH) template under metal-free and reagent-free conditions. They showed acetylene gas may undergo Diels-Alder [4+2]cycloaddition to the bay region of polycyclic aromatic hydrocarbon. Such cycloaddition at one of the bay regions at the tip of armchair (n,n) SWNT followed by rearomatization (dehydrogenation) adds a new aromatic six-membered ring along the tube axis. This group also predicted [19] that such a bottom-up process from a suitable small hydrocarbon template could be an environmentally friendly growth mechanism of larger diameter armchair tubes. It is worth mention that zigzag (m,0) SWNTs do not possess any bay region, which is advantageous as one kind of tube (i.e., armchair) can be grown using HCCH molecule.

Experimental studies [20-21] by Reinhoudt and co-researchers indicate that electron deficient acetylenes (ynamines) undergo [2+2]cycloaddition (under mild condition in apolar solvents) with electron rich alkenes (enamines) to form cyclobutenes. However, the MP2/6-31G* barrier height of 75 kcal/mol [22] of the reaction between unsubstituted acetylene and ethylene is not supportive of being observed experimentally. Based on this finding, it was concluded [22] that introduction of substituents may significantly lower the barrier height.

Since HBNH favors an unusual bond breaking/ring expansion reaction at the surface of BN nanotubes (smaller diameter) over commonly known [2+2]cycloaddition and there is a possibility of acetylene undergoing [2+2]cycloaddition with alkene, curiosity arises about the interaction between HCCH at the surface of SWNTs where carbon atoms are pseudo-sp2 hybridized (due to structural strain). Interestingly target tubes for cycloaddition by acetylene at the bay region of SWNT and bond cleavage/ring expansion by iminoborane at the surface of BNNTs differ significantly. The former process is favored in larger diameter SWNTs [19], while

the latter process works better for smaller diameter BNNTs. This difference in reactivity of HCCH and HBNH raises questions about the reaction between HCCH and smaller diameter SWNTs, as well as interaction between HBNH and smaller diameter SWNTs. Can acetylene break a C=C bond and form extended rings at the surface of SWNT? If so, then how stable are such complexes? Does HCCH, similar to HBNH, have any preference as to the chirality of the tube or interaction site, such as edge or middle of the tube? Does HBNH molecule behave similarly or differently while allowed to interact with SWNTs?

To address these tantalizing questions we employ density functional theory (DFT). In this context we also explored reactivity between HBNH and SWNTs, and HCCH with BNNTs. Thus the specific systems considered in the present investigation are HBNH-SWNT, HCCH-BNNT and HCCH-SWNT, and the results are compared with HBNH-BNNT [1]. For SWNT and BNNT, smaller diameter armchair (4,4) and zigzag (8,0) tubes were considered. The selection of smaller diameter tubes in the present investigation is also based on the recent finding that Diels-Alder functionalization disfavors [23] flat or weakly curved surfaces of carbon-based materials.

Method of calculations:

Periodic models are not appropriate for this study because such an approach cannot be applied to mimic edge functionalization due to interruption of translational symmetry. Thus, the molecular model seems a reasonable approach for this work. As representatives of armchair and zigzag tubes, (4,4) and (8,0) SWNT/BNNT, respectively, were chosen in the present investigation. These molecular models of tubes contain 64 carbon atoms in SWNTs, and 32 boron and 32 nitrogen atoms in BNNTs. Tips of both SWNT and BNNT were saturated with hydrogens to avoid dangling bonds.

The B3LYP variant of density functional theory (DFT) [24-25], was used to include correlation effects. A double-ζ quality 6-31G* basis set augmented with polarization spherical d-functions (5d) for all heavy atoms was used. (It may be noted that computational cost reduces by using 5d functions instead of 6d functions). Basis functions without a set of diffuse sp-functions for electronegative atoms are inadequate, especially for interaction energy. So an additional set of diffuse sp-functions was added to the 6-31G* basis function. Geometries of pristine and chemically modified SWNTs and BNNTs were fully optimized without any symmetry restriction using the 6-31+G* basis set, followed by vibrational analyses that insure the identification of true minima. To verify reliability of B3LYP results, additional calculations on some complexes were also performed using M06-2X [26].

Interaction energies (E_{Int}) refer to the energy difference between the complex and constituents and are obtained using the following equation (eq 1), where E refers to the electronic energy.

$$E_{Int} = E(\text{complex}) - (E(\text{SWNT/BNNT}) + E(\text{HBNH/HCCH}) \quad (1)$$

For an attractive or favorable interaction, the interaction energy is negative, repulsive forces are indicated by a positive quantity. All adsorption energies and activation energies are corrected for basis set superposition error (BSSE) using the counterpoise (CP) method [27].

All calculations were performed using the Gaussian-09 [28] code. Pristine nanotube models were obtained using TubeVBS software [29], and HCCH/HBNH molecules at different sites of C and BN tubes and terminal hydrogen atoms were initially positioned using Chemcraft [30] software, which is also used to generate figures and geometry analyses.

Results and Discussion

Several of the sites on the surface of the nanotubes which are available to interact with HCCH and HBNH are illustrated in Scheme 1, using BNNTs for illustrative purposes. First with respect to (4,4)-BNNT, sites A-C refer to BN bonds that lie perpendicular to the tube axis, while sites D and E represent diagonal BN orientations. With respect to (8,0)-BNNT, sites A, B and C, are diagonal while site D is parallel to the tube axis. Sites A, C and D of (4,4)-BNNT, and A and B of (8,0)-BNNT lie near the edges of the tubes, whereas the remaining sites, B and E of (4,4)-BNNT, and C and D of (8,0)-BNNT are positioned closer to the middle of the tubes. These same interaction sites were considered for complexation of HCCH and HBNH with SWNTs. In addition to all these sites, where HCCH or HBNH approach from above C=C or B=N bonds at the active sites, approach to the bay-region of (4,4) tubes (shown by the arrow in Scheme 1) were also investigated. That is two possible complex structures of armchair tubes were considered when guest molecule approaches site A from two different directions.

HBNH-(4,4)BNNT: First with regard to HBNH-(4,4)BNNT complexes [1], fully optimized geometries of (1A-1E) are displayed in the first row of Figure 1, along with BSSE-corrected B3LYP/6-31+G* (5d) binding energies. B=N bond cleavage/ring expansion takes place at sites A and B (BN bond perpendicular to the tube axis), bond cleavage at site C (also a perpendicular bond) and [2+2]cycloaddition at sites D and E (diagonal bond). Binding/interaction energy decreases in the order: 1A (-54.1) > 1B (-30,5) > 1C (-25.3) > 1D (-11.4) = 1E (-11.3). Based on these energies, clearly the bond cleavage/ring expansion processes (1A-1C) are considerably more favorable than the cycloaddition (1D and 1E) processes. Similar binding energies obtained by other methods (such as PBE0 and MP2) or expansion of basis set from 6-31+G* to 6-311++G** verifies [1] the reliability of B3LYP/6-31+G* to study such interactions.

In terms of the feasibility of the above reactions, the incorporation of HBNH into any of the tubes is expected to encounter a transition state and an associated energy barrier. The transition states (TS) of both bond cleavage/ring expansion and cycloaddition reactions were identified previously [1]. Transition state structures (1A-TS to 1E-TS) of all five reactions are displayed in the top row of Figure 2 where barrier heights of 11.8 to 14.2 kcal/mol indicate kinetically favorable reactions, where bond cleavage/ring expansion processes are a bit more favorable.

The perturbation in internal geometry of HBNH as a result of each reaction is in accord with the change from sp hybridization in HBNH to sp^2 in the complex. For example, the

B≡N bond distance of 1.24 Å stretches to 1.41 Å, close to the B=N distance of 1.40 Å in H_2BNH_2. Also the HBN/HNB angles change from 180º to around 120º, another indication of the transition from sp to sp^2 hybridization. As the interaction strength decreases from 1A to 1E, the BN bond distance of HBNH diminishes from 1.41 to 1.37 Å. Geometric parameters are also insensitive to the particular quantum chemical method (B3LYP vs PBE0).

Transition state structures (1A-1E in Figure 2) of HBNH-(4,4)BNNT reveal that the Lewis acidic sites [31], i.e., boron atoms, of the tube takes the leading role in both bond-breaking and cycloaddition processes. This conclusion is drawn from the geometric parameters within the TS, as in all cases, the B(tube) and N(HBNH) distances are shorter (by about 0.4 Å) than (B(HBNH)-N(tube) distances. This idea was also verified [1] by the intrinsic reaction coordinate (IRC) procedure [32]. This fact may be rationalized by examining the MOs where the lowest unoccupied MO (LUMO) of (4,4)-BNNT represents an antibonding p-orbital of the B atom, that accepts density from electron-rich sources to form a bond with B atom(s) of the tube.

HCCH-(4,4)BNNT: Somewhat different results are obtained when HBNH is replaced by HCCH. The fully optimized structures of HCCH-(4,4)BNNTs and their BSSE-corrected interaction energy are summarized in the second row (2A-2E) of Figure 1. Interestingly, the HCCH molecule follows its inorganic analogues while interacting at the perpendicular BN bonds (sites A-C). At these sites, HCCH also pulls apart the B=N bond of the tube and becomes an integral part of the tube by expanding the original hexagonal BN ring. However, these HCCH structures are less stable than the corresponding HBNH-(4,4)BNNT complexes. For example, the stabilization energy of 2A and 2B is lower by about 20 kcal/mol than the 1A and 1B structures of HBNH-(4,4)BNNT, while for 2C this decrement is about 7.0 kcal/mol. In comparison to edge sites 2A (-33.8 kcal/mol) and 2C (-18.4 kcal/mol), complex 2B (-9.6 kcal/mol) where HCCH approaches the middle of the tube surface is less stable. B3LYP interaction energies are in good agreement with M06-2X/6-31+G* values. For example, E_{Int} of 2A and 2C at the M06-2X level are -35.5 and -20.1 kcal/mol, respectively, changes of only 1.7 kcal/mol. As in the HBNH case, the change in internal geometry of HCCH is in accord with the change from sp hybridization in HCCH to sp^2 in the complex. For example, the C≡C bond distance of 1.21 Å stretches to ~1.34 Å in 2A-2C complexes, close to the CC double bond length.

The transition states for BN bond cleavage/ring expansion reactions to form 2A to 2C by HCCH were identified and each such TS includes a single imaginary vibrational frequency around ~530i cm^{-1} (Figure 2, second row). (It may be noted that the corresponding value is about 300i cm^{-1} in the TSs of 1A-1C). The TS geometries are displayed in the second-row of Figure 2, along with the BSSE-corrected barrier heights. Activation energies for the formation of 2A to 2C are around 36.0 kcal/mol, almost three times higher than for the corresponding HBNH complexes. In all three TS structures (2A-TS to 2C-TS), the (BNNT)B-C(C_2H_2) bond is shorter by about 0.4 Å than the (BNNT)N-C(C_2H_2) bond. The θ(HCC) bond angle (~142º), where the central carbon is closer to the B atom of the tube, is narrower by about 30º than the other CCH

angle (~170º) in the TSs of 2A-2C. This pattern suggests that the former C atom is approaching sp^2 hybridization as in H_2CCH_2, while the second one is still holding closer to sp hybridization in the transition states.

Interaction of HCCH at the diagonal B=N bond (either at the middle or at the edge) of (4,4)BNNT results in [2+2]cycloaddition products 2D and 2E in Figure 1. However, both structures are found unstable by about 16-17 kcal/mol relative to the separated species (note the positive values). On the contrary, the corresponding HBNH complexes are stabilized by about 11 kcal/mol, which represents a destabilization of ~28 kcal/mol when HBNH is replaced by HCCH. The activation energy (2D-TS and 2E-TS in Figure 2) for these two complexes is 39.1 kcal/mol. Thus, the [2+2]cycloaddition product of HCCH at the surface of BNNT, either at its middle or its edge, is thermodynamically unstable and the reaction is kinetically unfavorable. This finding is in accord with the finding that unsubstituted HCCH is reluctant to form such cycloaddition products.

The effects of extended BN/C network on the interaction energies of the [2+2]cycloaddition process have been estimated by comparing results with the simplest B=N/C=C bonded iminoborane/ethylene molecules. Reaction of the HCCH molecule with the B=N bond of H_2BNH_2 (Figure 3) barely alters the barrier height, lowered by only 2.0 kcal/mol from 39.0 kcal/mol in extended systems (2D and 2E) (Figure 3). However, the HCCH-H_2BNH_2 complex is found to be stable by about -5.1 kcal/mol at the same level of theory. This value is close to the energy of -5.5 kcal/mol obtained at the MP2/6-31+G(5d) level. In contrast, [2+2]cycloaddition of HBNH with H_2BNH_2 is favorable, as the resulting complex is stabilized by 26.4 kcal/mol (20.9 kcal/mol at the MP2 level) and lower barrier height of 13-14 kcal/mol. Thus, for the cycloaddition reaction, activation energies of armchair versions of both BNNT and SWNT is close to that of the corresponding simple molecules, but the extended system exhibits weaker complex structures. For example, the interaction energy of -11.4 kcal/mol in 1D is lower by 15 kcal/mol than in HBNH-H_2BNH_2. This same difference is roughly 22 kcal/mol comparing HCCH-SWNT (1D and 1E) with HCCH-H_2BNH_2, a change from endothermic in the extended carbon structure to an exothermic process in simple molecules.

For the armchair nanotubes, one more possibility is the interaction of HBNH/HCCH at the bay-region of the tubes. Optimized structures and BSSE corrected interaction energies of resulting complexes are exhibited in Figure 4. (Transition states could not be located for these reactions.) Based on the interaction energy, HBNH-(4,4)BNNT (5A) is stabilized by 6.2 kcal/mol, which is significantly lower (by about 48 kcal/mol) than the most stable structure 1A (Figure 1). In fact, all other possible isomers (1B-1E) are more stable than 5A, suggesting weak preference for the reaction at the bay-region. This reaction with HCCH is endothermic (E_{Int} = 19.4 kcal/mol) and will not result in a stable complex 5B.

HBNH-(4,4)SWNT: Interaction of HBNH with the all-carbon(4,4)SWNT follows similar patterns as described above for HBNH-BNNT and HCCH-BNNT, where the stabilities of the various HBNH-(4,4)SWNT complexes differ significantly. Structure 3A, where HBNH is

attached to site A, is the most stable of these complexes (3A-3E). The interaction energy of 3A (-44.9 kcal/mol) is intermediate between that of 1A (-54.1 kcal/mol) and 2A (-33.8 kcal/mol). The BSSE corrected E_{Int} of 9.2 kcal/mol (5C in Figure 4) clearly does not support complex formation at the bay-region. Although complexation of HBNH with SWNT at site A (3A) is quite favorable, the reaction exhibits a high activation energy of 36.0 kcal/mol (3A-TS in Figure 2), similar to that of HCCH-BNNT (2A-TS in Figure 2).

The stability of 3B (E_{Int} = -2.4 kcal/mol), where HBNH is attached to the middle perpendicular bond of SWNT (site B), is about 1/12 that of 1B, and ¼ of 2B. Moving to site C, again a perpendicular bond but at the edge, increases the stability of 3C to -10.1 kcal/mol, less stable than 1C and 2C. The barrier height of 44.1 kcal/mol (3B-TS) is slightly higher than that of 2B-TS. However, the formation of 3C is slightly more favorable (32.4 kcal/mol vs. 35.1 kcal/mol) kinetically than 2C.

Similar to HCCH-(4,4)BNNT, both diagonal sites (D and E, Scheme 1) of SWNT are not favorable for an incoming HBNH molecule. Ensuing complexes are unstable by 14-25 kcal/mol, with the interaction energy at the edge site (3D) lower than that of the middle site (3E). Both reactions involve a high barrier of about 42-46 kcal/mol. Comparison of energies of HBNH-H_2CCH_2 (Figure 3) indicates that extension of carbon network strongly disfavors the [2+2]cycloaddition process in SWNT. For example, the binding energy of -20.1 kcal/mol in HBNH-H_2CCH_2 changes to 14-25 kcal/mol in HBNH-SWNT complexes (3D and 3E), and the barrier height increases by about 20 kcal/mol.

HCCH-(4,4)SWNT: The optimized structures and BSSE-corrected interaction energies of HCCH-(4,4)SWNT are reported in the last row of Figure 1. Acetylene forms its most stable complex 4A (E_{Int} = -59.9 kcal/mol) with SWNT and forms an octagon at the edge (site A). The activation energy of this C=C bond breaking and ring expansion process is about 38 kcal/mol. Approaching the bay-region, instead from the top of C=C bond at the site A, lowers the binding energy to 0.5 kcal/mol (Figure 4). This finding of an almost unbound structure 5D suggests smaller diameter armchair tubes may not be grown by [4+2]cycloaddition of HCCH at the bay-region, as predicted by the Scott group [19] due to possible high activation energy. Rather, acetylene may prefer to create an octagon-defect near the edge.

Acetylene is found to form a stable complex when allowed to interact at sites B and C, where the latter structure (4C) is slightly more stable than 4B. Geometric parameters at the active site of 4C are close to that of HCCH-H_2CCH_2 (Figure 3), suggesting a possible [2+2]cycloaddition product. The other two structures 4D and 4E are unstable by 5 and 18 kcal/mol, respectively. In comparison to the simplest HCCH-H_2CCH_2 complex, extended structure 4C in this case, is destabilized by about 11 kcal/mol.

Although 4A is energetically a very stable complex, the activation energy of 38.0 kcal/mol for its formation is rather high. Almost the same activation energy occurs for structure 4B. Cycloaddition product 4C and HCCH-H_2CCH_2 exhibit similar activation energy of 47 kcal/mol. An even higher barrier is predicted for the formation of 4D and 4E.

In summary, all three perpendicular-to-axis sites of armchair BNNT/SWNT are favorable for complexation with both HBNH and HCCH, with different amounts of stability. Site A of both BNNT and SWNT is the most favorable site for either HCCH or HBNH, when they approach from top of the bond. Interaction energy follows the order: HCCH-SWNT (-59.9 kcal/mol) > HBNH-BNNT (-54.1 kcal/mol) > HBNH-SWNT (-44.9 kcal/mol) > HCCH-BNNT (-33.8 kcal/mol). The bay-region is found not suitable for either HBNH or HCCH.

Structurally all four of the most stable complexes (1A, 2A, 3A and 4A) exhibit similar patterns: B=N/C=C breaks and adsorbate become an integral part of the tube by expanding from hexagon to octagon where HBNH/HCCH unit resides above the surface. Formation of these complexes also depends on the activation energy. In the case of HBNH-BNNT, the barrier height of 12 kcal/mol supports the feasibility of such a reaction. However, in the other three cases reaction has to overcome a barrier of about 36-38 kcal/mol. A similar activation energy is found when HCCH approaches the bay-region of armchair tubes and PAH [19] and it has been suggested that substituted acetylenes most likely reduce the barrier height, so one might expect the same for present cases. In that case, RBNR'/RCCR' (R, R' =functional groups) may be added to the tube surface to synthesize several functionalized BNNT/SWNT nanotubes. The synthesis of either all BN or all CC as well as hybrid BN-CC and CC-BN structures may thus exhibit a wide range of properties.

The next favorable site is again at the edge (site C) and follows similar stability pattern as found in site A. Stability of HBNH-BNNT and HCCH-SWNT is higher than the hybrid HBNH-SWNT and HCCH-BNNT structures. With the exception of HCCH-BNNT, all other structures form what may be described as [2+2]cycloaddition products. The least stable complexes are those where HCCH/HBNH resides at the middle (site B), except HBNH-BNNT. Although structurally they are similar, energetically hybrid complexes are less stable. So it can be said that interaction with the same group of elements (B/N or C) are more favorable than the mixed complex. This may be due to variation of bond polarity (B=N vs C=C) and better π-conjugation within the same group of elements, such as HBNH-BNNT and HCCH-SWNT.

The activation energies of these reactions at sites B and C are quite high, and substituted HBNH and HCCH may reduce the barrier to establish a favorable process. Interestingly, the B atom of BNNT at the active sites takes an active role in TS formation in HBNH-BNNT and HCCH-BNNT, reflected in shorter B(BNNT)-N(HBNH) and B(BNNT)-C(HCCH) distances than N(BNNT)-B(HBNH) and N(BNNT)-C(HCCH) bond distances. In the case of SWNT, B of HBNH approaches first to the SWNT. These findings are true for all TS structures.

HBNH-(8,0)BNNT: The key features of interactions of the HBNH molecule at different sites (Scheme 1) of (8,0)BNNT, published earlier [1], are summarized here. Structures, relevant geometric parameters and BSSE corrected interaction energies of HBNH-(8,0)BNNTs are displayed in the top row of Figure 5. Contrary to armchair tube, BN bond cleavage/ring expansion takes place at the diagonal BN sites (site A-C, 6A-6C in Figure 5) and [2+2]cycloaddition is preferred at the parallel site (site D, 6D in Figure 5). Complexes 6A and

6B of the first kind are more stable (by about 30 kcal/mol) than the cycloaddition product 6D. However, bond cleavage at the middle diagonal B=N bond (as in 6C) is less favorable than the edge sites, and 6C is energetically close to 6D. In fact, 6C is intermediate between bond cleavage/ring expansion and cycloaddition. In comparison with the most stable (1A, -54.1 kcal/mol) structure of HBNH-armchair tube, the most stable zigzag tube complex (6A, -44.0 kcal/mol) exhibits a reduced binding energy by about 10 kcal/mol.

Similar BN bond lengths (1.43-1.47 Å) at the active region of 6A and 6B, including the iminoborane section, indicate delocalization of π-electrons in the octagon as in borazine. Whereas the BN bond length of the guest HBNH in 6C and 6D structures is close to the B=N distance of 1.40 Å as in H_2BNH_2, connecting BN bonds are longer (> 1.5 Å), indicating single B-N bonds. This pattern suggests π-delocalization is a key factor in stabilizing structures 6A and 6B.

In addition to greater stability, activation energies (shown in the first row of Figure 6) of the formation of 6A (6A-TS, 9.4 kcal/mol) and 6B (6B-TS, 7.5 kcal/mol) are lower than that of 6C (6C-TS, 15.6 kcal/mol) and 6D (6D-TS, 14.1 kcal/mol). This factor clearly suggests favorability of complexation in former over latter complexes. In the transition states of HBNH-(8,0)BNNT (Figure 6) the boron atom of the tube first forms a bond with N of HBNH in both processes. This is reflected in the shorter B(tube)-N(HBNH) distance than N(tube)-B(HBNH), and the θ(HNB) angle is narrower than θ(HBN) angle, where the latter angle is still close to 180º.

HCCH-(8,0)BNNT: Complexes formed by the interaction between HCCH and BNNT are illustrated in the second row of Figure 5, with corresponding transition state structures in Figure 6. Similar to HBNH, HCCH also breaks a diagonal B=N bond at the edges (7A and 7B) and expands a hexagonal BN ring to an octagonal ring that includes two carbon atoms of HCCH. Both structures exhibit the same binding energy of -16.0 kcal/mol (-17.0 kcal/mol at the M06-2X level) energy but are less stable by more than 25 kcal/mol than their all-BN 6A and 6B counterparts. Moving the HCCH molecule to the middle diagonal B=N site from edge sites yields an unstable complex 7C by 8.2 kcal/mol. Change of the site to a parallel B=N bond site (site D) further lowers the interaction energy to 17.8 kcal/mol. So the reactivity of HCCH differs from HBNH while interacting with the BNNT, interaction energies lowered significantly for acetylene than inorganic cousin. Still complexation at the edges are favorable while unfavorable at the middle. This difference may be due to weaker π-delocalization between C=C and BN hexagon than that of B=N with BN hexagon.

Thus in a mixture of both (4,4)BNNT and (8,0)BNNT, HCCH would prefer the former tube at the perpendicular B=N bond at site A (complex 2A, E_{Int} = -34 kcal/mol) followed by a B=N bond at the other edge site (2C, E_{Int} = -18.4 kcal/mol) which is slightly more stable (by about 2 kcal/mol) than the most stable 7A and 7B complexes of zigzag BN-tube. However, a high activation energy of about 40 kcal/mol for 7B formation, more than 4 times that of 6A or 6B, would hinder the reaction. We could not precisely identify a TS for 7A as SCF convergence could not be achieved in one of the steps of the transition state geometry optimization, but one

might presume an activation energy for 7A similar to that found in 7B-TS. Structural parameters of all transition states indicate that the boron atom of the tube takes a leading role as the B-C distances (~1.8 Å) are shorter than N-C bonds (~2.1 Å). Thus, derivatives of HCCH may lower the barrier height as well as the stability of these complexes.

HBNH-(8,0)SWNT: Switching positions of adsorbate and adsorbent, discussed in the previous section, also leads to a similar binding energy pattern. Complex 8A (Figure 5), where the edge diagonal C=C bond site hosting HBNH breaks and lengthens, is stabilized by -13.6 kcal/mol. It may be noted that for (8,0)SWNT there is no difference between sites A and B. Sites C and D, both at the middle of the tube, form cycloaddition products. However, positive binding energy of 10.3 kcal/mol for 8C and 25.4 kcal/mol for 8D are not supportive of complexation at these sites. However, the energy difference between 8C and 8D indicates complexation at the diagonal C=C bond is likely preferred over parallel bond, and derivatives of HBNH may stabilize the 8C complex. A transition state for 8A could not be located, but the high activation energy for 8C (36 kcal/mol) and 8D (42 kcal/mol) complex formation would hinder the process.

HCCH-(8,0)SWNT: Interaction between HCCH and (8,0)SWNT resulted in stable complex 9A (Figure 5) where the C=C bond of the tube at site A is broken by HCCH and the ring is expanded from hexagon to octagon. The energy of formation of complex 9A is -31.6 kcal/mol, which is lower (by 12 kcal/mol) than formation of 6A from HBNH and (8,0)BNNT. Other two structures 9C and 9D are found unstable by 7.6 and 11.8 kcal/mol, respectively. Activation energies of 16.1 kcal/mol (Figure 6) indicate bond breaking/ring expansion to form 9A may be realized experimentally. While the TS for 9C could not be located, a high barrier (about 52.5 kcal/mol) rules out formation of cycloaddition product 9D. Interestingly, the barrier height of the reaction between HCCH and H_2CCH_2 to form cycloaddition product cyclobutene HCCH-H_2CCH_2 (Figure 3) is close to that of the extended system (9D), whereas stability of the simple 4-ring product is three times greater than in the extended system.

In summary, both bond breaking/ring expansion and cycloaddition products are possible when HBNH and HCCH are allowed to react at the surface of zigzag tubes. Reactions are more favorable (both thermodynamically and kinetically) at the edge site to expand the ring at the tip of the tube. All BN (HBNH-zigzag-BNNT) or all C (HCCH-zigzag-SWNT) systems are found to be much more stable than the hybrid systems (HBNH-zigzag-SWNT and HCCH-zigzag-BNNT). Except for HBNH-(8,0)BNNT systems, most of the cycloaddition products are energetically unstable by low magnitude, with a high energy barrier impeding their formation. This situation may be reversible to form a stable complex by considering derivatives of HCCH and HBNH.

Conclusions:

Interaction between BNNTs and HBNH resulted in most stable complexes and both bond breaking/ring expansion and [2+2]cycloaddition processes are favorable kinetically. Similar to iminoborane (HBNH), acetylene (HCCH) is also able to selectively modify the surface of small diameter BNNTs (both (4,4) armchair and (8,0) zigzag tubes), either at their edge sites or middle sites. Unlike HBNH, HCCH only undergoes B=N/C=C bond breaking/ring expansion process, where selectivity of sites is followed as in its inorganic analogue. Kinetically complex formation, where guest and host comprise the same set of elements, are much more favorable than hybrid compositions. Contrary to the favorable [2+2]cycloaddition HBNH-BNNT products, formation of such complexes by HCCH at the surface of BNNT/SWNT is not favorable, mostly due to high activation energy. A similar unfavorable situation is encountered when SWNTs are the host for the HBNH molecule.

Favorable complexation by acetylene at the edge sites of both kinds of SWNTs seems possible, where (4,4)-SWNT-HCCH complexes are more stable than the (8,0)-SWNT-HCCH complexes. However, a high barrier represents a kinetic hurdle for such complexation process. It may be possible to lower this activation energy by introducing substituents to make one carbon center of HCCH more electron-rich, as the interaction first takes place with the Lewis acid center, i.e., B atoms of the tubes.

This theoretical investigation indicates possibilities for modifying both BNNT and SWNT at their surface by both HBNH and HCCH. Stability of complexes and low activation energies of the bond breaking and ring expansion process suggest complexation may be realized experimentally. If activation energies can be controlled by introducing substituent(s) at HCCH and HBNH then [2+2]cycloaddition products may be realized. However, it is worth mentioning that only smaller diameter tubes may be modified at their surface, but not wider tubes and flat sheets.

Acknowledgements

TK is thankful to Alexander von Humboldt Foundation for financial support. Computational facilities at Utah State University and DoD HPC at AFRL (Dayton, USA) are gratefully acknowledged.

References

(1) Sundaram, R.; Scheiner, S.; Roy, A. K.; Kar, T., B═N Bond Cleavage and BN Ring Expansion at the Surface of Boron Nitride Nanotubes by Iminoborane. *J. Phys. Chem. C* **2015**, *119*, 3253-3259.

(2) Paetzold, P., Iminoboranes. *Adv. Inorg. Chem.* **1987**, *31*, 123-170.

(3) Paetzold, P., New Perspectives in Boron - Nitrogen Chemistry - I. *Pure & Appl. Chem* **1991**, *63*, 345-350.

(4) Müller, M.; Maichle-Mössmer, C.; Bettinger, H. F., BN-Phenanthryne: Cyclotetramerization of an 1,2-Azaborine Derivative. *Angew. Chem. Int. Ed.* **2014**, *53*, 9380–9383.

(5) Bettinger, H. F.; Müller, M., Pathways for the Cyclotetramerization of Dibenz[C,E][1,2]Azaborine, a BN-Phenanthryne. *J. Phys. Org. Chem.* **2015**, *28*, 97-103.

(6) Chopra, N. G.; Luyken, R. J.; Cherrey, K.; Crespi, V. H.; Cohen, M. L.; Louie, S. G.; Zettl, A., Boron Nitride Nanotubes. *Science* **1995**, *269*, 966-967.

(7) Terrones, M.; Hsu, W. K.; Terrones, H.; Zhang, J. P.; Ramos, S.; Hare, J. P.; Castillo, R.; Prasside, K.; Cheetham, A. K.; Kroto, H. W., et al., Metal Particle Catalysed Production of Nanoscale Bn Structures. *Chem. Phys. Lett.* **1996**, *259*, 568-573.

(8) Loiseau, A.; Willaime, F.; Demoncy, N.; Hug, G.; Pascard, H., Boron Nitride Nanotubes with Reduced Numbers of Layers Synthesized by Arc Discharge. *Phys. Rev. Lett.* **1996**, *76*, 4737-4740.

(9) Terauchi, M.; Tanaka, M.; Takehisa, M.; Saito, Y., Electron Energy-Loss Spectroscopy Study of the Electronic Structure of Boron Nitride Nanotubes. *J. Electron Microsc.* **1998**, *47*, 319-324.

(10) Laude, T.; Matsui, Y.; Marraud, A.; Jouffrey, B., Long Ropes of Boron Nitride Nanotubes Grown by a Continuous Laser Heating. *App. Phys. Lett.* **2000**, *76*, 3239-3241.

(11) Golberg, D.; Bando, Y.; Sato, T.; Grobert, N.; Reyes-Reyes, M.; Terrones, H.; Terrones, M., Nanocages of Layered Bn: Super-High Presure Nanocells for Formation of Solid Nitrogen. *J. Chem. Phys.* **2002**, *116*, 8523-8532.

(12) Golberg, D.; Bando, Y.; Huang, Y.; Terao, T.; Mitome, M.; Tang, C.; Zhi, C., Boron Nitride Nanotubes and Nanosheets. *ACS Nano* **2010**, *4*, 2979-2993.

(13) Zhong, G.; Hofmann, S.; Yan, F.; Telg, H.; Warner, J. H.; Eder, D.; Thomsen, C.; Milne, W. I.; Robertson, J., Acetylene: A Key Growth Precursor for Single-Walled Carbon Nanotube Forests. *J. Phys. Chem. C* **2009**, *113*, 17321-17325.

(14) Prasek, J.; Drbohlavova, J.; Chomoucka, J.; Hubalek, J.; Jasek, O.; Adam, V.; Kizek, R., Methods for Carbon Nanotubes Synthesis-Review. *J. Mater. Chem.* **2011**, *21*, 15872-15884.

(15) Omachi, H.; Nakayama, T.; Takahashi, E.; Segawa, Y.; Itami, K., Initiation of Carbon Nanotube Growth by Well-Defined Carbon Nanorings. *Nat Chem* **2013**, *5*, 572-576.

(16) Fort, E. H.; Jeffreys, M. S.; Scott, L. T., Diels-Alder Cycloaddition of Acetylene Gas to a Polycyclic Aromatic Hydrocarbon Bay Region. *Chem. Commun.* **2012**, *48*, 8102-8104.

(17) Fort, E. H.; Donovan, P. M.; Scott, L. T., Diels−Alder Reactivity of Polycyclic Aromatic Hydrocarbon Bay Regions: Implications for Metal-Free Growth of Single-Chirality Carbon Nanotubes. *J. Am. Chem. Soc.* **2009**, *131*, 16006-16007.

(18) Scott, L. T., Polycyclic Aromatic Hydrocarbon Bowls, Baskets, Balls, and Tubes: Challenging Targets for Chemical Synthesis. *Polycyclic Aromatic Compounds* **2010**, *30*, 247-259.
(19) Fort, E. H.; Scott, L. T., Carbon Nanotubes from Short Hydrocarbon Templates. Energy Analysis of the Diels–Alder Cycloaddition/Rearomatization Growth Strategy. *J. Mater. Chem.* **2011**, *21*, 1373-1381.
(20) Pennings, M. L. M.; Reinhoudt, D. N., Chemistry of Four-Membered Cyclic Nitrones. 1. Synthesis and Thermal Isomerization of 2,3-Dihydroazete 1-Oxides. *J. Org. Chem.* **1982**, *47*, 1816-1823.
(21) Verboom, W.; Visser, G. W.; Trompenaars, W. P.; Reinhoudt, D. N.; Harkema, S.; van Hummel, G. J., Synthesis of Pyrrolizines by Intramolecular Capture of 1,4-Dipolar Intermediates in Reactions of Enamines with Dimethyl Acetylenedicarboxylate. *Tetrahedron* **1981**, *37*, 3525-3533.
(22) Andes Hess JR., B.; Schaad, L. J.; Reinhoudt, D. N., [2 + 21 Cycloadditions. A Concerted Pathway for Acetylene Plus Ethylene *Intern. J. Quantum Chem.* **1986**, *XX1X*, 345-350.
(23) Willocq, B.; Lemaur, V.; El Garah, M.; Ciesielski, A.; Samori, P.; Raquez, J. M.; Dubois, P.; Cornil, J., The Role of Curvature in Diels-Alder Functionalization of Carbon-Based Materials. *Chem. Commun.* **2016**, *52*, 7608-7611.
(24) Becke, A. D., Density-Functional Thermochemistry. III. The Role of Exact Exchange. *J. Chem. Phys.* **1993**, *98*, 5648-5652.
(25) Lee, C.; Yang, W.; Parr, R. G., Development of the Colle-Salvetti Correlation-Energy Formula into a Functional of the Electron Density,. *Phys, Rev. B* **1988**, *37*, 785-789.
(26) Zhao, Y.; Truhlar, D. G., The M06 Suite of Density Functionals for Main Group Thermochemistry, Thermochemical Kinetics, Noncovalent Interactions, Excited States, and Transition Elements: Two New Functionals and Systematic Testing of Four M06-Class Functionals and 12 Other Functionals. *Theor. Chem. Acc.* **2008**, *120*, 215-241.
(27) Boys, S. F.; Bernardi, F., The Calculation of Small Molecular Interactions by the Differences of Separate Total Energies. Some Procedures with Reduced Errors. *Mol. Phys.* **1970**, *19*, 553-566.
(28) Frisch, M. J.; Trucks, G. W.; Schlegel, H. B.; Scuseria, G. E.; Robb, M. A.; Cheeseman, J. R.; Scalmani, G.; Barone, V.; Mennucci, B.; Petersson, G. A., et al., *Gaussian09*; Gaussian, Inc., Wallingford CT, USA, 2009.
(29) Veiga, R. G. A.; Tomanek, D., Tubevbs (http://k.1asphost.com/Tubeasp/Tubevbs.Html). **2007**.
(30) Zhurko, G. A., http://www.chemcraftprog.com.
(31) Sundaram, R.; Scheiner, S.; Roy, A. K.; Kar, T., Site and Chirality Selective Chemical Modifications of Boron Nitride Nanotubes (BNNTs) Via Lewis Acid/Base Interactions. *Phys. Chem. Chem. Phys* **2015**, *17*, 3850-3866.
(32) Fukui, K., The Path of Chemical-Reactions - the IRC Approach. *Acc. Chem. Res.* **1981**, *14*, 363-368.

Figure Captions:

Figure 1. B3LYP/6-31+G* structures and key geometric parameters of (4,4)BNNT-HBNH (1A-1E), (4,4)BNNT-HCCH (2A-2E), (4,4)SWNT-HBNH (3A-3E) and (4,4)SWNT-HCCH (4A-4E). Color scheme: B – yellow, N – blue, C – larger gray sphere and H – smaller gray sphere. Bond lengths are in Angstrom and angles in degree. BSSE corrected interaction energies in kcal/mol. Negative interaction energy means stable complex, otherwise unstable. HCCH unit in 4A is shown by arrow.

Figure 2. B3LYP/6-31+G* transition state (TS) structures and key geometric parameters of (4,4)BNNT-HBNH (1A-TS -1E-TS), (4,4)BNNT-HCCH (2A-TS - 2E-TS), (4,4)SWNT-HBNH (3A-TS - 3E-TS) and (4,4)SWNT-HCCH (4A-TS - 4E-TS). Color scheme: B – yellow, N – blue, C – larger gray sphere and H – smaller gray sphere. Bond lengths are in Angstrom and angles in degree. BSSE corrected barrier heights are in kcal/mol, and imaginary frequency is in cm-1.

Figure 3. B3LYP/6-31+G* ground and transition state (TS) structures of cycloaddition products. Distances in Angstrom and angles in degree. BSSE corrected interaction energies and BSSE corrected activation energies (B3LYP/6-31+G*, MP2/6-31+G*) are in kcal/mol.

Figure 4. B3LYP/6-31+G* ground state structures where HBNH/HCCH approached at the bay-region (shown by arrow) of BNNT and SWNT. Distances in Angstrom and angles in degree. BSSE corrected interaction energies are in kcal/mol. See Figure 1 for atom's color scheme.

Figure 5. B3LYP/6-31+G* structures and key geometric parameters of (8,0)BNNT-HBNH (6A-6D), (8,0)BNNT-HCCH (7A-7D), (8,0)-HBNH (8A-8D) and (8,0)-HCCH (9A-9D). Color scheme: B – yellow, N – blue, C – larger gray sphere and H – smaller gray sphere. Bond lengths are in Angstrom and angles in degree. BSSE corrected interaction energies in kcal/mol. Negative interaction energy means stable complex, otherwise unstable. HCCH group in 9A is shown by arrow.

Figure 6. B3LYP/6-31+G* transition state (TS) structures and key geometric parameters of (8,0)BNNT-HBNH (5A-TS -5D-TS), (8,0)BNNT-HCCH (6B-TS – 6D-TS), (8,0)SWNT-HBNH (7C-TS, 7D-TS) and (4,4)SWNT-HCCH (8A-TS – 8D-TS). Color scheme: B – yellow, N – blue, C – larger gray sphere and H – smaller gray sphere. Bond lengths are in Angstrom and angles in degree. BSSE corrected barrier heights are in kcal/mol and imaginary frequencies in cm-1.

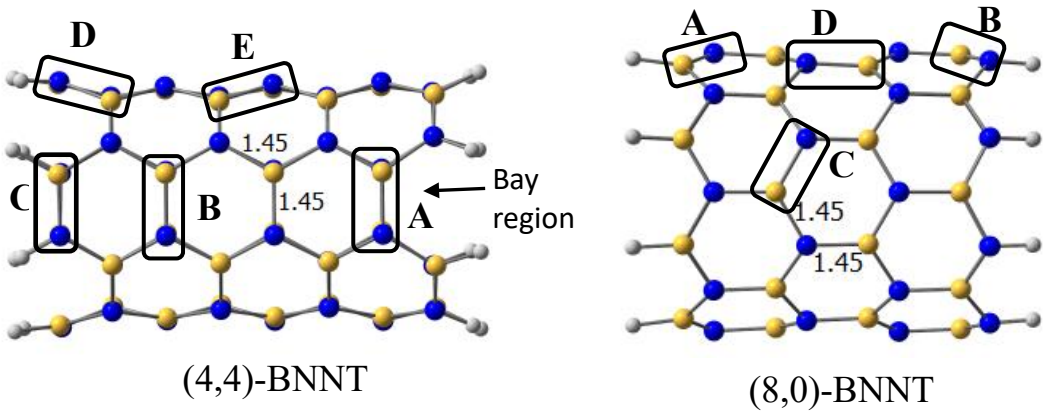

Scheme 1. Active sites of (4,4) and (8,0) BNNTs. Blue, yellow and grey colors represent N, B and H atoms, respectively. Bond lengths are in Å. Bay region of (4,4) tube is shown by arrow.

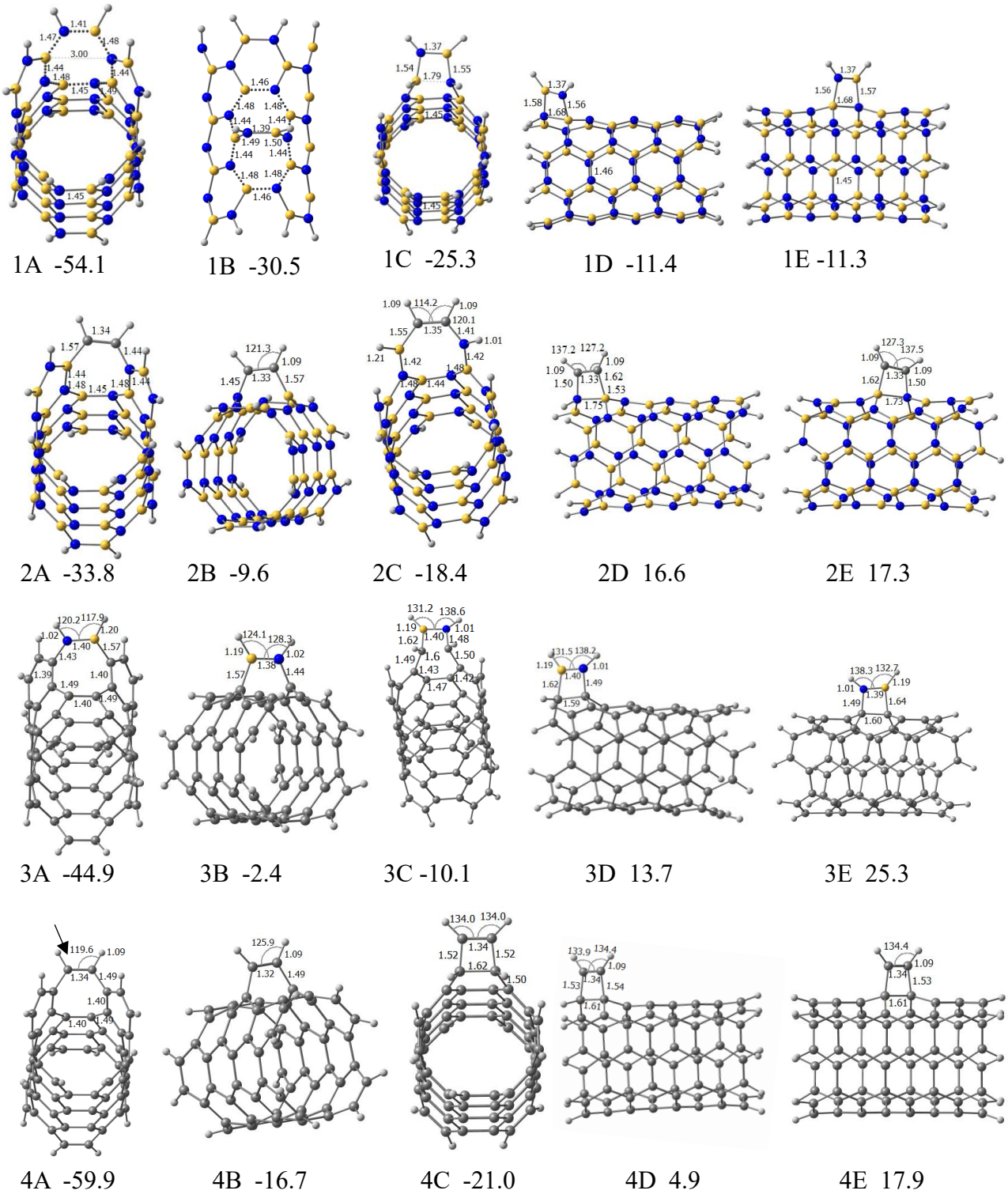

Figure 1. B3LYP/6-31+G* structures and key geometric parameters of (4,4)BNNT-HBNH (1A-1E), (4,4)BNNT-HCCH (2A-2E), (4,4)SWNT-HBNH (3A-3E) and (4,4)SWNT-HCCH (4A-4E). Color scheme: B – yellow, N – blue, C – larger gray sphere and H – smaller gray sphere. Bond lengths are in Angstrom and angles in degree. BSSE corrected interaction energies in kcal/mol. Negative interaction energy means stable complex, otherwise unstable. HCCH unit in 4A is shown by arrow.

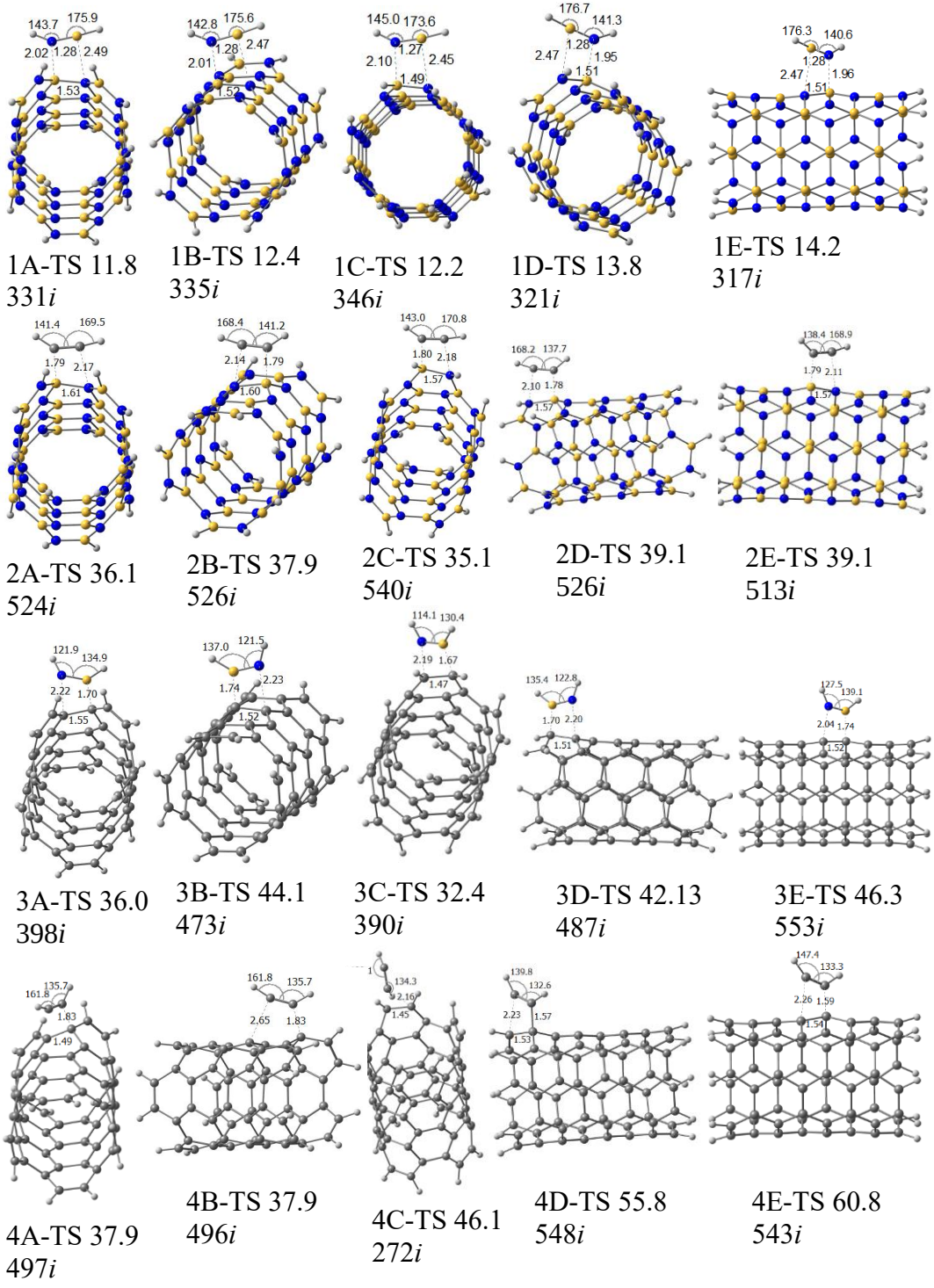

Figure 2. B3LYP/6-31+G* transition state (TS) structures and key geometric parameters of (4,4)BNNT-HBNH (1A-TS -1E-TS), (4,4)BNNT-HCCH (2A-TS - 2E-TS), (4,4)SWNT-HBNH (3A-TS - 3E-TS) and (4,4)SWNT-HCCH (4A-TS - 4E-TS). Color scheme: B – yellow, N – blue, C – larger gray sphere and H – smaller gray sphere. Bond lengths are in Angstrom and angles in degree. BSSE corrected barrier heights are in kcal/mol, and imaginary frequency is in cm^{-1}.

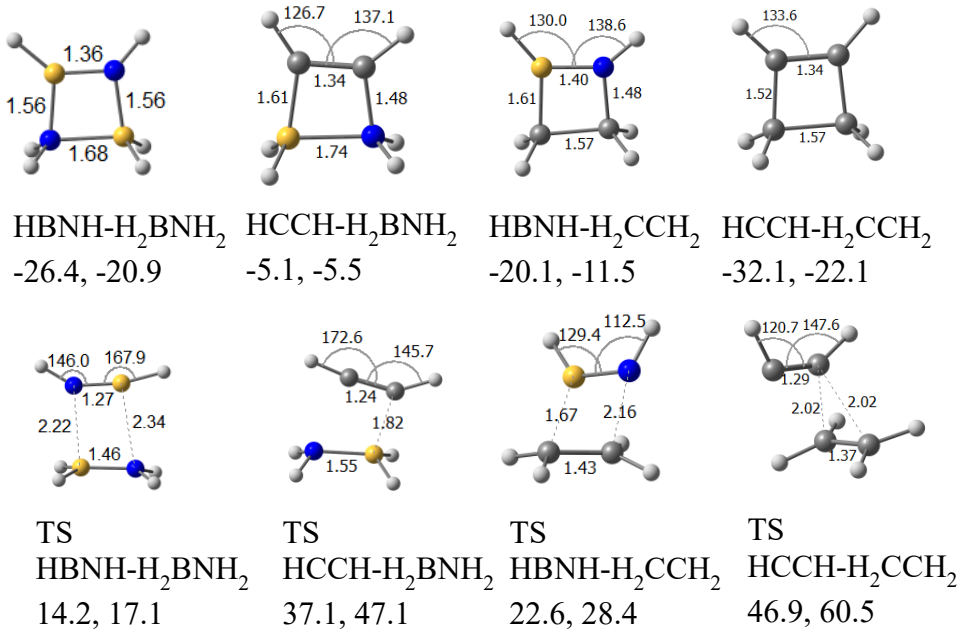

Figure 3. B3LYP/6-31+G* ground and transition state (TS) structures of cycloaddition products. Distances in Angstrom and angles in degree. BSSE corrected interaction energies and BSSE corrected activation energies (B3LYP/6-31+G*, MP2/6-31+G*) are in kcal/mol.

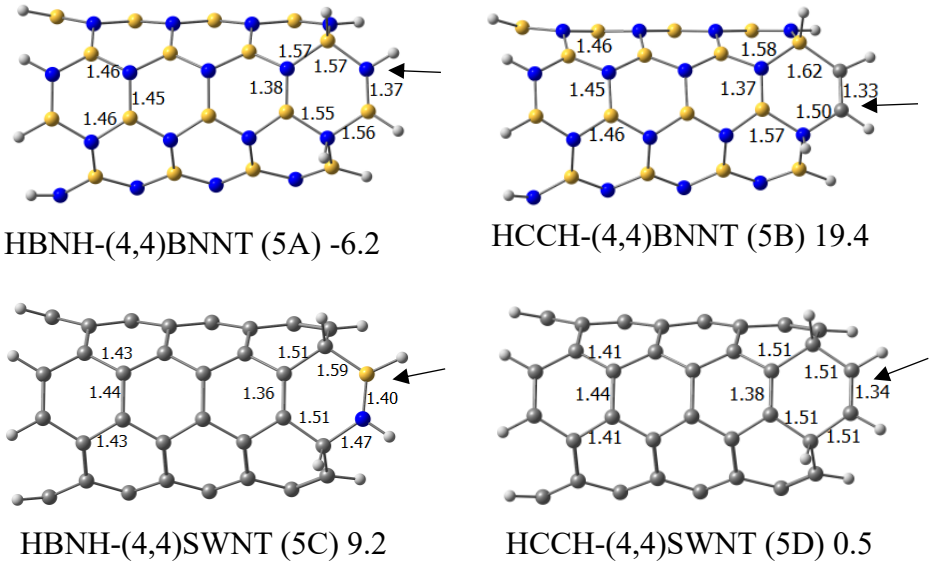

Figure 4. B3LYP/6-31+G* ground state structures where HBNH/HCCH approached at the bay-region (shown by arrow) of BNNT and SWNT. Distances in Angstrom and angles in degree. BSSE corrected interaction energies are in kcal/mol. See Figure 1 for atom's color scheme.

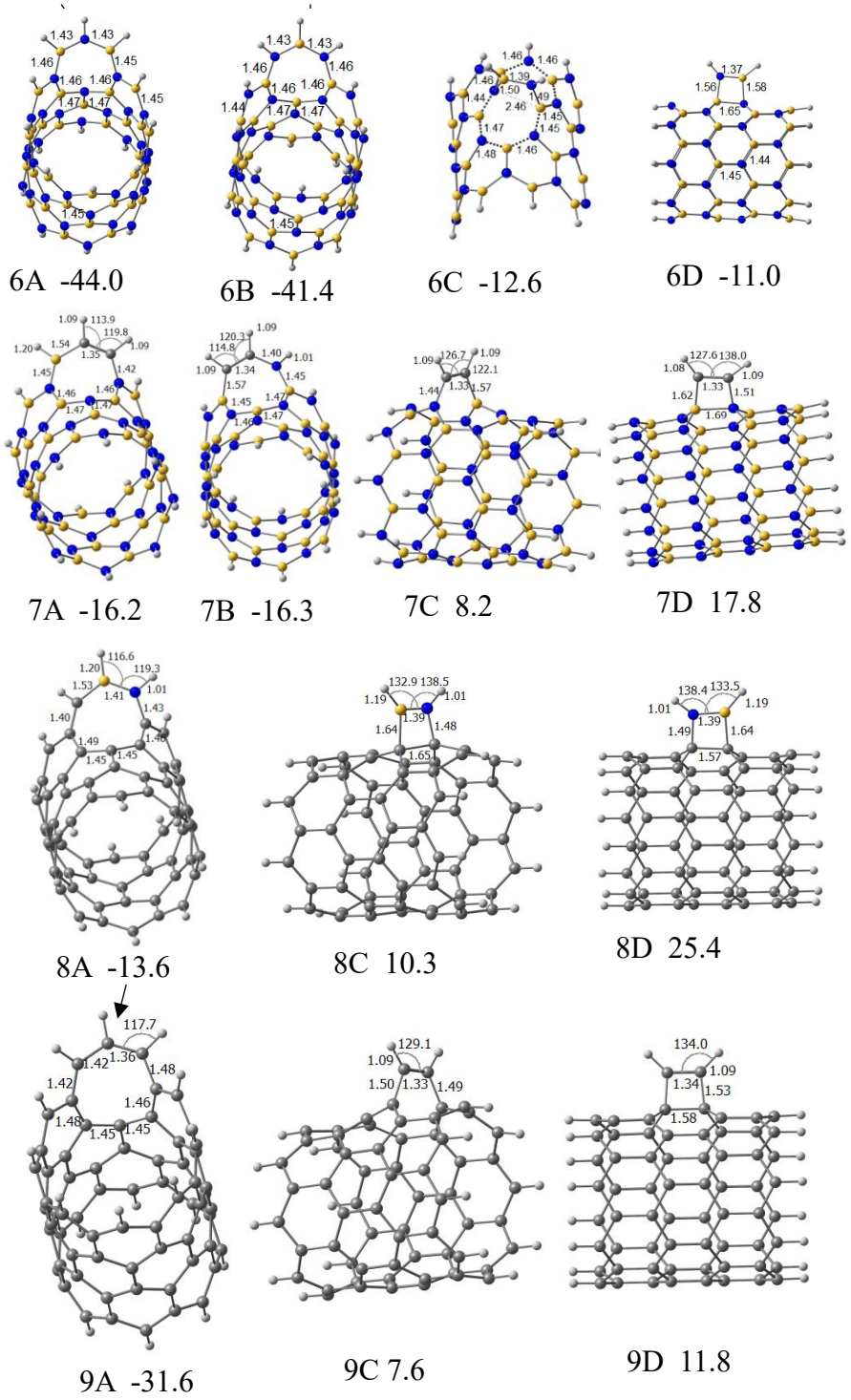

Figure 5. B3LYP/6-31+G* structures and key geometric parameters of (8,0)BNNT-HBNH (6A-6D), (8,0)BNNT-HCCH (7A-7D), (8,0)-HBNH (8A-8D) and (8,0)-HCCH (9A-9D). Color scheme: B – yellow, N – blue, C – larger gray sphere and H – smaller gray sphere. Bond lengths are in Angstrom and angles in degree. BSSE corrected interaction energies in kcal/mol. Negative interaction energy means stable complex, otherwise unstable. HCCH group in 9A is shown by arrow.

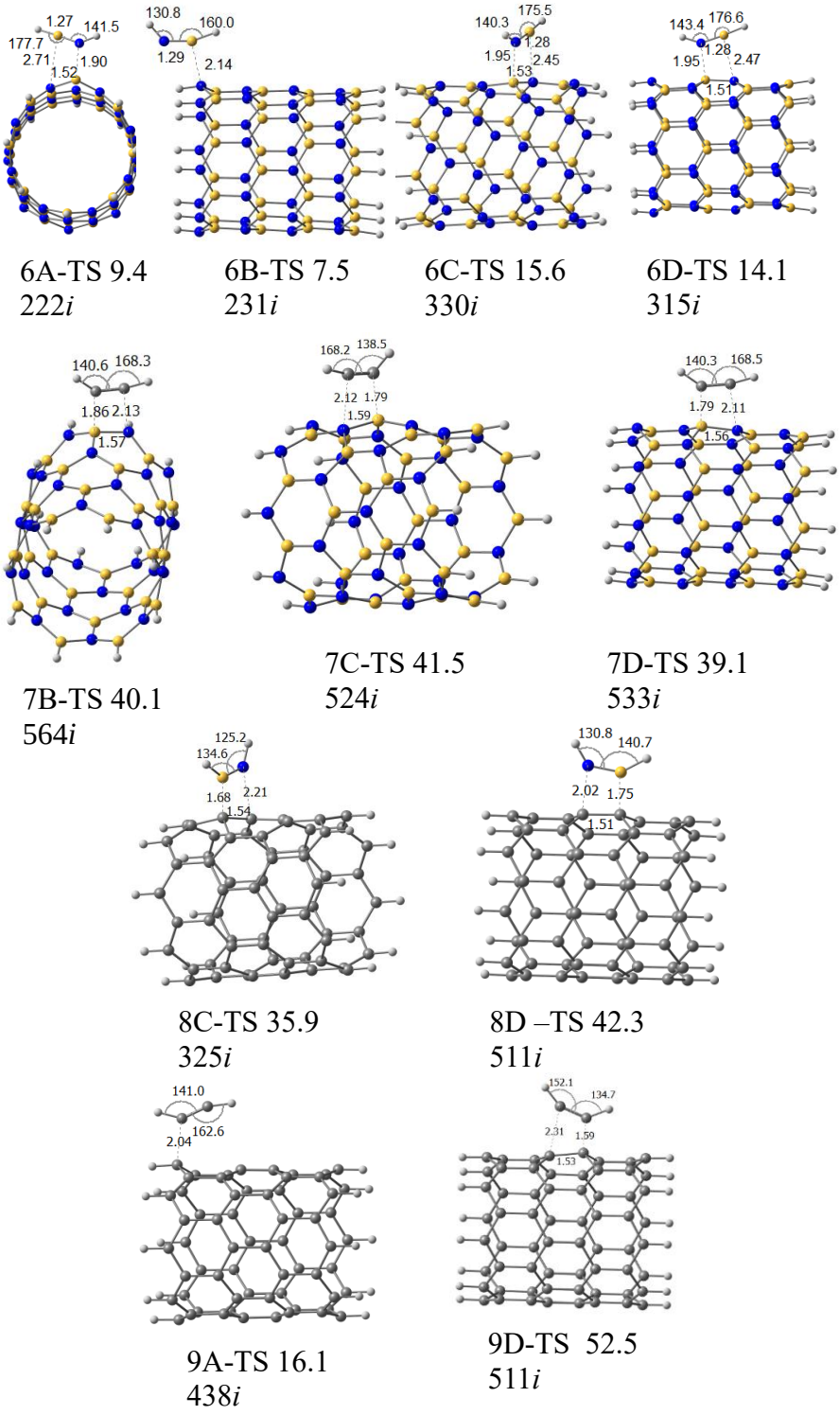

Figure 6. B3LYP/6-31+G* transition state (TS) structures and key geometric parameters of (8,0)BNNT-HBNH (5A-TS -5D-TS), (8,0)BNNT-HCCH (6B-TS – 6D-TS), (8,0)SWNT-HBNH (7C-TS, 7D-TS) and (4,4)SWNT-HCCH (8A-TS – 8D-TS). Color scheme: B – yellow, N – blue, C – larger gray sphere and H – smaller gray sphere. Bond lengths are in Angstrom and angles in degree. BSSE corrected barrier heights are in kcal/mol and imaginary frequencies in cm^{-1}.